ANALYSIS OF SMALL-SCALE WRINKLE RIDGES IN AEOLIS DORSA, MARS. R. M. Borden[1] and D. M. Burr[1], [1]University of Tennessee, Knoxville, TN USA 37996 (rborden4@vols.utk.edu and dburr1@utk.edu).

Introduction: Wrinkle ridges are common tectonic features on terrestrial planetary bodies, including Earth, Mercury, the Moon, and Mars [1,2]. On Mars, they are mainly found on volcanic plains, and the largest ones, measuring hundreds or even thousands of kilometers in length, are related to the Tharsis Montes and Olympus Mons [3,4]. Wrinkle ridges are interpreted to be formed by tectonic compression [2], and thus Martian wrinkle ridges can be used to make inferences about the tectonic history of Mars on both global and regional scales.

The Aeolis Dorsa (AD) region of Mars is a sedimentary basin located on the global dichotomy boundary. Several small-scale wrinkle ridges have previously been observed in this area [5]. We have mapped the wrinkle ridges in AD and are now using their morphology and orientations to infer the contractional tectonic history of this region.

Background:

Aeolis Dorsa region: The Aeolis Dorsa sedimentary basin is located between two plana: Aeolis Planum on the west and Zephyria Planum on the east (Figure 1).

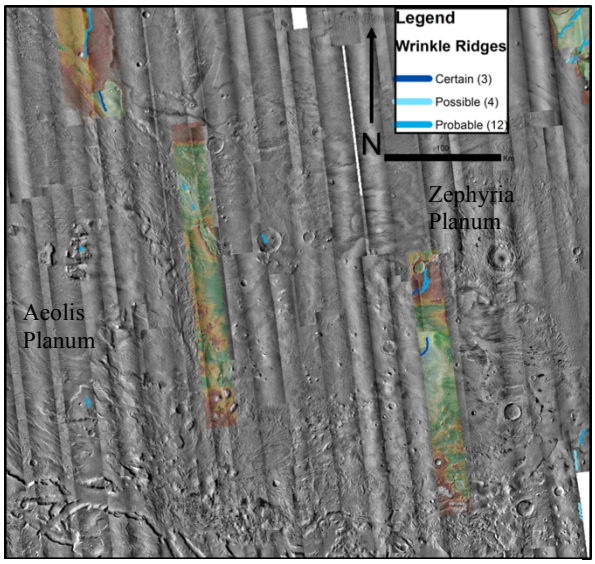

Figure 1: Mapped wrinkle ridges in the Aeolis Dorsa mapping area. Figure background is a CTX mosaic, with colored CTX DEMs. Colored lines denote certainty levels: dark blue denotes certain, medium blue denotes probable, and light blue denotes possible (see Table 1). Black scale bar below legend is 100 km.

Multiple geologic processes have influenced the current surface geomorphology in the region, as evidenced by fluvial, volcanic, and aeolian landforms [5-8].

Wrinkle ridges: Wrinkle ridges are commonly comprised of three main geomorphologic parts: a low underlying topographic rise, a broad arch, and a narrower crenulated ridge (the "wrinkle") on top [9]. However, not all parts are observed on all ridges, possibly due either to lithology or preservation state. They are also commonly asymmetric, having a steeper slope on one side of the ridge, although the sense of asymmetry may change side along strike. Wrinkle ridges sometimes consist of en echelon segments, where one ridge contains several segments that are parallel and offset. These segments are attributed to rotation of the stress field during wrinkle ridge formation [10].

The commonly accepted formation mechanism of wrinkle ridges is as anticlinal folds formed by slip along blind thrust faults [11]. Based on this interpretation, it is possible to use wrinkle ridges to find the amount of shortening and direction of the maximum principal compressive stress at the time of ridge formation. The integrated length of a transverse topographic profile across a ridge minus the straight-line length of the same profile will give the amount of shortening due to folding across the ridge [12]. The amount of shortening from faulting can be estimated by using the measured elevation offset on either side of the ridge and an assumed fault dip (a value of ~30^{o} was used by [4]). The geographic orientation of a ridge can be taken as perpendicular to the direction of greatest compression, and thus the direction of the maximum principal compressive stress can be derived [13].

Hypothesis: Based on this background information on wrinkle ridges and previous observations of wrinkle ridges in Aeolis Dorsa [5], the following hypotheses have been used for this work:

Null hypothesis: The Aeolis Dorsa region underwent contraction that was the same throughout the region (regional control on the stress direction). The evidence supporting this hypothesis would be wrinkle ridges with a single strong preferred orientation or with a pattern of orientations consistent with a single geographic location as the origin of deformation.

Alternate hypothesis: The Aeolis Dorsa region underwent contraction that was more localized and not controlled at the regional level. The evidence supporting this hypothesis would be ridges across AD without a preferred orientation and/or with random orientations.

Data and Methods:

Mapping: For this project, we mapped wrinkle ridges in the Aeolis Dorsa region at 1:100,000 scale using a mosaic of images from the Context Camera (6m/px; CTX) [14] on the Mars Reconnaissance Orbiter. The CTX image mosaic was overlain by Mars Orbiter Laser Altimeter (MOLA) [15] data to allow for

easier identification of features while mapping. In addition to wrinkle ridges, this region also contains several other types of ridge features: sinuous ridges interpreted as inverted fluvial deposits [6 and references therein], yardangs from Aeolian erosion [7], and dunes from Aeolian deposition [8 and references therein]. Because of the abundance of other (non-tectonic) ridges in the AD region, we used several criteria, based on the literature on wrinkle ridges, to provide levels of certainty in our mapping (Table 1). For example, their asymmetry [4] helps to distinguish them from other types of ridges in the AD mapping area, which do not show asymmetry.

Mapping Criteria	Certainty		
	Certain	Probable	Possible
Profile view: 1.Topographic rise 2. Asymmetry	2 of 2 profile criteria needed	1 of 2 profile criteria needed	1 of 2 profile criteria needed
Map view: 1. Narrow ridge 2. En echelon segments 3. Curvilinear shape 4. Broad arch	3 of 4 map view criteria needed	3 of 4 map view criteria needed	2 of 4 map view criteria needed

Table 1: Criteria used to determine certainty levels of mapped wrinkle ridges.

With the mapping, we collected the location, orientation, and length of each ridge using ArcMap. Where stereo pair CTX images overlie wrinkle ridges, we made Digital Elevation Models (DEMs) using Ames Stereo Pipeline software [16], resulting in detailed topographic information on 12 of 19 mapped wrinkle ridges. From these DEMs, ~30 topographic profiles were taken across each ridge and used to measure their heights and widths, as well as the elevation offset on either side of each ridge.

Analyses. The resultant data were analyzed in several ways. First, the orientations of all of the wrinkle ridges were made into a rose diagram using the GeoRose software program [17]. This rose diagram was used to determine the preferred orientation of the wrinkle ridges in AD. Integrated lengths of topographic profiles for each ridge were used, along with the straight-line length of the profiles, to determine the shortening from folding. The elevation offset was used to determine the amount of shortening from faulting for an assumed fault dip of ~30^0 [4].

Results: Mapping has resulted in identification of 19 wrinkle ridges: 3 Certain, 12 Probable, and 4 Possible (Figure 1). The orientation data show a NE-SW preferred orientation (centered around 35°), indicating an orthogonal direction of maximum principal compressive stress oriented NW-SE. Shortening from folding ranges from ~8-160 m (~0.5-6° of ridge width), while shortening from faulting ranges from ~25-176 m (~0.5-11.

Discussion and Implications: The presence of the wrinkle ridges implies slippage along thrust faults, consistent with an interpretation of the host Medusae Fossae Formation as layered [e.g., 18]. The small amount of shortening for these wrinkle ridges suggests that the compressive stresses were either short-lived or weak or that the material being compressed was relatively strong. The NW-SE orientation of the maximum principal stress is unexpected. Along the WNW-ESE-oriented highland-lowland boundary in southern AD, tectonic deformation may have resulted from lower crustal flow [19] or from lithospheric flexure, e.g., due to surface loading [20 and references therein]. However, the resultant compressive stresses would have been oriented NNE-WSW, almost orthogonal to the compressive stresses inferred in this work. This mismatch, along with their small size, suggests some other origin for the contraction that produced the AD wrinkle ridges.

Future work: The measured dimensions and shortening across the ridges from the topographic profiles will be used to calculate ratios of displacement/length and width/height. These ratios will be used to compare these ridges with the much larger wrinkle ridges on the volcanic plains of Mars, using data from previous studies. A clustering analysis of the locations of the wrinkle ridges will be completed and a statistical analysis of the wrinkle ridge orientations to determine its modality. The results of these analyses will will provide constraints on the origin(s) of the compressive stress(es) that formed these AD features.

References: [1] Watters T. R. (1988) *JGR, 93*, 10234-10236. [2] Plescia J. B. and Golombek M. P. (1986) *GSA Bulletin, 97,* 1289-1299. [3] Golombek M. P. and Phillips R. J. (2010) *Planetary Tectonics,* 183-232. [4] Golombek M. P. et al. (2001) *JGR, 106,* 23811-23821. [5] Kite E. S. et al. (2015) *Icarus, 253,* 223-242. [6] Jacobsen R. E. and Burr D. M. (2017) *Geosphere, 13 (6).* [7] Ward A. W. (1979) *JGR, 84(B14),* 8147-8166. [8] Boyd A. S. and Burr D. M (2016) *Planetary Mappers Meeting*, Flagstaff, AZ. [9] Lucchitta B. K. (1977) *Proceedings of LSC,* 2691-2703. [10] Smart K. J. et. al. (2006) *LPSC 37, #1966.* [11] Mueller K. and Golombek M. P. (2004) *Ann. Rev. of EPS, 32,* 435-464. [12] Golombek M. P. et. al. (1991) *Proceedings of LPSC 21*, 679-693. [13] Anderson E. M. (1951) *The Dynamics of Faulting.* [14] Malin M. C. et al. (2007), *JGR, 112,* E05S04. [15] Smith D. E. et al. (2001) *JGR, 106,* 23689-23722. [16] Moratto Z. M. (2010) *LPS XLI,* Abstract #2364. [17] Yong Technology Inc. (2014). GeoRose. Edmonton, Canada. http://www.yongtechnology.com/download/georose [18] Bradley B. A. et al. (2002) *JGR, 107,* 2-1-2-17. [19] Nimmo F. (2005) *Geology, 33,* 533-536. [20] Lefort A. et al. (2015) *Geomorphology, 240,* 121-136.